

Lattice Boltzmann Model for High-Order Nonlinear Partial Differential Equations

Baochang Shi* and Nanzhong He†
*School of Mathematics and Statistics,
 Huazhong University of Science and Technology,
 Wuhan 430074, People's Republic of China*

Zhaoli Guo‡
*State Key Laboratory of Coal Combustion,
 Huazhong University of Science and Technology,
 Wuhan 430074, People's Republic of China
 (Dated: September 13, 2018)*

A general lattice Boltzmann (LB) model is proposed for solving nonlinear partial differential equations with the form $\partial_t \phi + \sum_{k=1}^m \alpha_k \partial_x^k \Pi_k(\phi) = 0$, where α_k are constant coefficients, and $\Pi_k(\phi)$ are the known differential functions of ϕ , $1 \leq k \leq m \leq 6$. The model can be applied to the common nonlinear evolutionary equations, such as (m)KdV equation, KdV-Burgers equation, $K(m, n)$ equation, Kuramoto-Sivashinsky equation, and Kawahara equation, etc. Unlike the existing LB models, the correct constraints on moments of equilibrium distribution function in the proposed model are given by choosing suitable *auxiliary-moments*, and how to exactly recover the macroscopic equations through Chapman-Enskog expansion is discussed in this paper. Detailed simulations of these equations are performed, and it is found that the numerical results agree well with the analytical solutions and the numerical solutions reported in previous studies.

PACS numbers: 02.70.-c, 02.60.Cb, 05.45.Yv

I. INTRODUCTION

The lattice Boltzmann method (LBM) is a promising technique for simulating fluid flows and modeling complex physics in fluids [1, 2, 3]. Compared with the conventional computational fluid dynamics approaches, the LBM is easy for programming, intrinsically parallel, and it is also easy to include complicated boundary conditions such as those in porous media. Up to now, the most widely used LBM is the so-called lattice Bhatnagar-Gross-Krook (LBGK) model. However, the LBGK model may suffer from numerical instability when it is used to simulate the fluid with small viscosity. A lot of work has been done to improve the stability of LB model, among which the multi-relaxation-time LBM [4, 5, 6] and entropic LBM [7, 8, 9, 10, 11] have attracted much attention in recent years. It should be noted that the LBM also shows potentials to simulate the nonlinear systems, such as the reaction-diffusion equation [12, 13, 14], convection-diffusion equation (CDE) [15, 16, 17, 18], Burgers equation [19], KdV-like equation [20], Poisson equation [21], etc. Recently, the LB models have been extended to solve CDEs on rectangular or irregular lattices [22, 23] and anisotropic dispersion equations [24, 25, 26], among which the model proposed by Ginzburg [26] is generic.

Except for solving real-valued nonlinear systems, the LB and LB-like models have been successful in solving complex-valued nonlinear systems. Since the middle of 1990s, several types of quantum lattice gases and quantum LBM have been proposed based on quantum-computing ideas to model some real and complex mathematical-physical equations, such as the Schrödinger equation, Gross-Pitaevskii equation, Burgers equation, KdV equation [27, 28, 29, 30, 31, 32, 33, 34, 35, 36], etc. We refer the readers to a recent paper [36] for a detailed review. On the other hand, recently the classical LB model has been used to model complex-valued equations. In Ref. [37] the LBM was applied to one-dimensional (1D) nonlinear Schrödinger equation (NLSE) following the idea of quantum lattice-gas model [30, 31] to treat the reaction term. In Ref. [38], motivated by the work in Ref. [37], the LBM for n -dimensional (n D) CDE with a source term was directly applied to some nonlinear complex equations, including the NLSE, coupled NLSEs, Klein-Gordon equation and coupled Klein-Gordon-Schrödinger equations, by adopting a complex-valued distribution function and relaxation time. In Ref. [39], a general LB model for a class of n D nonlinear CDEs was presented by properly selecting equilibrium distribution function. The model in Ref. [39] can be applied to both real and complex-valued nonlinear evolutionary equations. Following the idea in Ref. [39], a LB model for 1D nonlinear Dirac equation

*Electronic address: shibc@hust.edu.cn

†Electronic address: nzhe@hust.edu.cn

‡Electronic address: zlguo@hust.edu.cn

was given in Ref. [40], which is of second-order accuracy in both space and time, and the order of accuracy is near 3.0 at lower grid resolution. The studies in Refs. [37, 38, 39, 40] show that the LBM may be an effective numerical solver for real and complex-valued nonlinear systems.

Most of the existing LB models are used for solving partial differential equations (PDEs) with order lower than or equal to three, while many efficient conventional numerical methods for solving higher-order PDEs have been proposed, such as the pseudo-spectral method [41], local discontinuous Galerkin (LDG) method [42, 43], finite difference scheme [44], finite volume method [45], radial basis function method [46], among them LDG method has attracted much attention due to its good nature, such as flexibility and high parallel efficiency (see a recent review article [43] and references therein for details). Although some higher-order LB schemes have been proposed, they are mainly limited to solve lower-order PDEs [47, 48, 49] and 1D special problems [50]. Furthermore, the efficient numerical analysis of these schemes are still needed. Therefore, it is important to research and develop the LB model for solving higher-order PDEs.

In this paper, by extending the idea in Ref. [39] a general LBGK model is proposed for solving a class of nonlinear partial differential equations (NPDEs) with order up to six. In order to exactly recover the macroscopic NPDE, the correct constraints on moments of equilibrium distribution function in the proposed model are given by introducing suitable *auxiliary-moments*. The proposed model can be used to solve many common nonlinear evolutionary equations, such as (m)KdV equation, KdV-Burgers equation, K(m, n) equation, Kuramoto-Sivashinsky equation, and Kawahara equation, etc. Numerical results show that the LBGK model can also be used to simulate higher-order NPDEs.

The rest of the paper is organized as follows. In Sec. II, the LBGK model for NPDE is presented, and how to exactly recover the macroscopic equation from the model is discussed. In Sec. III, the equilibrium distribution and auxiliary-moment functions for NPDEs with different orders are given. Numerical tests of the LBGK model are made in Sec. IV, and finally a brief summary is given in Sec. V.

II. MULTI-SCALE LATTICE BOLTZMANN EQUATIONS

A. LBGK Model

The 1D NPDE considered in this paper can be written as

$$\partial_t \phi + \sum_{k=1}^m \alpha_k \partial_x^k \Pi_k(\phi) = 0, \quad (1)$$

where ϕ is a scalar function of position x and time t , $\alpha_1 = 1$, α_k are constant coefficients, and $\Pi_k(\phi)$ are known differential functions of ϕ , $1 \leq k \leq m \leq 6$.

Our LBGK model is based on the D1Q b lattice [2] with b velocity directions in 1D space. The evolution equation of the distribution function in the model reads

$$f_j(x + c_j \Delta t, t + \Delta t) = f_j(x, t) - \frac{1}{\tau} [f_j(x, t) - f_j^{\text{eq}}(x, t)], \quad (2)$$

where $\{c_j, j = 0, \dots, b-1\} \subseteq \{0, c, -c, 2c, -2c, 3c, -3c\}$ is the set of discrete velocity directions, $c = \Delta x / \Delta t$, Δx and Δt are lattice spacing and time step, respectively, τ is the dimensionless relaxation time, and $f_j^{\text{eq}}(x, t)$ is the equilibrium distribution function (EDF).

To solve Eq. (1) using Eq. (2), we must give appropriate EDF $f_j^{\text{eq}}(x, t)$. By applying the idea in Ref. [39] to the higher-order NPDE (1), the following constrains on f_j^{eq} are given

$$\begin{aligned} \sum_j f_j &= \sum_j f_j^{\text{eq}} = \phi, \quad \sum_j c_j f_j^{\text{eq}} = \Pi_1, \\ \sum_j c_j^k f_j^{\text{eq}} &= \Pi_{k0} + \beta_k \Pi_k, \quad k = 2, \dots, m \end{aligned} \quad (3)$$

where β_k are parameters, and Π_{k0} are *auxiliary-moment* (AM) functions for correctly recovering Eq. (1), which are determined later, $k = 2, \dots, m$.

B. Multi-Scale Lattice Boltzmann Equations

To derive the macroscopic equation (1), the Chapman-Enskog (C-E) expansion in time and space is applied:

$$f_j = \sum_{k=0}^6 \epsilon^k f_j^{(k)}, \partial_t = \sum_{k=1}^6 \epsilon^k \partial_{t_k}, \partial_x = \epsilon \partial_{x_1}, \quad (4)$$

where ϵ is a small expansion parameter. Using the first formula in Eq. (3) and Eq. (4), we have

$$\sum_j f_j^{(k)} = 0, k \geq 1. \quad (5)$$

By applying Taylor expansion to Eq. (2), we get

$$D_j f_j + \frac{\Delta t}{2} D_j^2 f_j + \dots + \frac{\Delta t^5}{720} D_j^6 f_j + \dots = -\frac{1}{\tau \Delta t} (f_j - f_j^{\text{eq}}), \quad (6)$$

where $D_j = \partial_t + c_j \partial_x$. Denote $D_{1j} = \partial_{t_1} + c_j \partial_{x_1}$. Similar to Ref. [47], substituting Eq. (4) into Eq. (6) and treating the terms in order of ϵ^k separately gives

$$f_j^{(0)} = f_j^{\text{eq}}, \quad (7)$$

$$D_{1j} f_j^{(0)} = -\frac{1}{\tau \Delta t} f_j^{(1)}, \quad (8)$$

$$\partial_{t_2} f_j^{(0)} + \tau_2 \Delta t D_{1j}^2 f_j^{(0)} = -\frac{1}{\tau \Delta t} f_j^{(2)}, \quad (9)$$

$$\partial_{t_3} f_j^{(0)} + 2\tau_2 \Delta t \partial_{t_2} D_{1j} f_j^{(0)} + \tau_3 \Delta t^2 D_{1j}^3 f_j^{(0)} = -\frac{1}{\tau \Delta t} f_j^{(3)}, \quad (10)$$

$$\partial_{t_4} f_j^{(0)} + 2\tau_2 \Delta t \partial_{t_3} D_{1j} f_j^{(0)} + 3\tau_3 \Delta t^2 \partial_{t_2} D_{1j}^2 f_j^{(0)} + \tau_2 \Delta t \partial_{t_2}^2 f_j^{(0)} + \tau_4 \Delta t^3 D_{1j}^4 f_j^{(0)} = -\frac{1}{\tau \Delta t} f_j^{(4)}, \quad (11)$$

$$\begin{aligned} & \partial_{t_5} f_j^{(0)} + 2\tau_2 \Delta t \partial_{t_4} D_{1j} f_j^{(0)} + 3\tau_3 \Delta t^2 \partial_{t_2}^2 D_{1j} f_j^{(0)} + 3\tau_3 \Delta t^2 \partial_{t_3} D_{1j}^2 f_j^{(0)} \\ & + 2\tau_2 \Delta t \partial_{t_2} \partial_{t_3} f_j^{(0)} + 4\tau_4 \Delta t^3 \partial_{t_2} D_{1j}^3 f_j^{(0)} + \tau_5 \Delta t^4 D_{1j}^5 f_j^{(0)} = -\frac{1}{\tau \Delta t} f_j^{(5)}, \end{aligned} \quad (12)$$

$$\begin{aligned} & \partial_{t_6} f_j^{(0)} + 2\tau_2 \Delta t \partial_{t_5} D_{1j} f_j^{(0)} + 6\tau_3 \Delta t^2 \partial_{t_2} \partial_{t_3} D_{1j} f_j^{(0)} + 3\tau_3 \Delta t^2 \partial_{t_4} D_{1j}^2 f_j^{(0)} + 2\tau_2 \Delta t \partial_{t_2} \partial_{t_4} f_j^{(0)} + 6\tau_4 \Delta t^3 \partial_{t_2}^2 D_{1j}^2 f_j^{(0)} \\ & + \tau_3 \Delta t^2 \partial_{t_2}^3 f_j^{(0)} + \tau_2 \Delta t \partial_{t_3}^2 f_j^{(0)} + 4\tau_4 \Delta t^3 \partial_{t_3} D_{1j}^3 f_j^{(0)} + 5\tau_5 \Delta t^4 \partial_{t_2} D_{1j}^4 f_j^{(0)} + \tau_6 \Delta t^5 D_{1j}^6 f_j^{(0)} = -\frac{1}{\tau \Delta t} f_j^{(6)}, \end{aligned} \quad (13)$$

where

$$\begin{aligned} \tau_2 &= -\tau + \frac{1}{2}, \\ \tau_3 &= \tau^2 - \tau + \frac{1}{6}, \\ \tau_4 &= -\tau^3 + \frac{3}{2}\tau^2 - \frac{7}{12}\tau + \frac{1}{24}, \\ \tau_5 &= \tau^4 - 2\tau^3 + \frac{5}{4}\tau^2 - \frac{1}{4}\tau + \frac{1}{120}, \\ \tau_6 &= -\tau^5 + \frac{5}{2}\tau^4 - \frac{13}{6}\tau^3 + \frac{3}{4}\tau^2 - \frac{31}{360}\tau + \frac{1}{720}. \end{aligned} \quad (14)$$

C. Recovery of the Third-Order NPDE

Since general LB models for the second-order NPDE have been developed [26, 39], we only discuss how to recover NPDEs with orders higher than two in this paper. Summing Eqs. (8) and (9) over j , and using Eqs. (3) and (5), we obtain

$$\sum_j D_{1j} f_j^{(0)} = \partial_{t_1} \phi + \partial_{x_1} \Pi_1(\phi) = 0, \quad (15)$$

$$\partial_{t_2} \phi + \tau_2 \Delta t \sum_j D_{1j}^2 f_j^{(0)} = 0. \quad (16)$$

Using Eqs. (3) and (15), and taking Π_{20} as in Ref. [39] such that $\partial_{t_1}\Pi_1 + \partial_{x_1}\Pi_{20} = 0$, that is $\Pi_{20} = \int \partial_\phi \Pi_1 \partial_\phi \Pi_1 d\phi$, we have

$$\sum_j D_{1j}^2 f_j^{(0)} = \partial_{t_1}^2 \phi + 2\partial_{t_1} \partial_{x_1} \Pi_1 + \partial_{x_1}^2 (\Pi_{20} + \beta_2 \Pi_2) = \partial_{x_1} (\partial_{t_1} \Pi_1 + \partial_{x_1} \Pi_{20}) + \beta_2 \partial_{x_1}^2 \Pi_2 = \beta_2 \partial_{x_1}^2 \Pi_2, \quad (17)$$

then it follows from Eqs. (16) and (17) that

$$\partial_{t_2} \phi + \alpha_2 \partial_{x_1}^2 \Pi_2 = 0, \quad (18)$$

with $\alpha_2 = \Delta t \tau_2 \beta_2$.

Summing Eq. (10) over j , and using Eqs. (3), (5), (15) and (17), we obtain

$$\partial_{t_3} \phi + \tau_3 \Delta t^2 \sum_j D_{1j}^3 f_j^{(0)} = 0, \quad (19)$$

$$\begin{aligned} \sum_j D_{1j}^3 f_j^{(0)} &= \partial_{t_1}^3 \phi + 3\partial_{t_1}^2 \partial_{x_1} \Pi_1 + 3\partial_{t_1} \partial_{x_1}^2 (\Pi_{20} + \beta_2 \Pi_2) + \partial_{x_1}^3 (\Pi_{30} + \beta_3 \Pi_3) \\ &= 2\partial_{t_1}^2 \partial_{x_1} \Pi_1 + 3\partial_{t_1} \partial_{x_1}^2 (\Pi_{20} + \beta_2 \Pi_2) + \partial_{x_1}^3 (\Pi_{30} + \beta_3 \Pi_3) \\ &= \partial_{x_1}^2 (\partial_{t_1} (\Pi_{20} + 3\beta_2 \Pi_2) + \partial_{x_1} \Pi_{30}) + \beta_3 \partial_{x_1}^3 \Pi_3. \end{aligned} \quad (20)$$

If we take Π_{30} such that $\partial_{t_1} (\Pi_{20} + 3\beta_2 \Pi_2) + \partial_{x_1} \Pi_{30} = 0$, that is,

$$\Pi_{30} = \int \partial_\phi (\Pi_{20} + 3\beta_2 \Pi_2) \partial_\phi \Pi_1 d\phi = \int [(\partial_\phi \Pi_1)^3 + 3\beta_2 \partial_\phi \Pi_2 \partial_\phi \Pi_1] d\phi, \quad (21)$$

then from Eqs. (19) and (20), we have

$$\partial_{t_3} \phi + \alpha_3 \partial_{x_1}^3 \Pi_3 = 0, \quad (22)$$

with $\alpha_3 = \Delta t^2 \tau_3 \beta_3$.

Combining Eqs. (15), (18) and (22), the third-order NPDE is exactly recovered to order $O(\epsilon^3)$

$$\partial_t \phi + \partial_x \Pi_1(\phi) + \alpha_2 \partial_x^2 \Pi_2(\phi) + \alpha_3 \partial_x^3 \Pi_3(\phi) = 0, \quad (23)$$

with $\alpha_2 = \Delta t \tau_2 \beta_2, \alpha_3 = \Delta t^2 \tau_3 \beta_3$.

Remark 1. Note that there are no additional assumptions on the present model for the third-order NPDEs with the form of Eq. (1), and if we select Π_{20} and Π_{30} above the third-order NPDEs are exactly recovered. The present model with a D1Q4 or D1Q5 lattice can be used to simulate the third-order NPDE (1) which contains some KdV-type equations.

D. Recovery of the Fourth-Order NPDE

Summing Eq. (11) over j , and using Eqs. (3), (5), (15), (17) and (20), we obtain

$$\partial_{t_4} \phi + 3\tau_3 \Delta t^2 \partial_{t_2} \partial_{x_1}^2 (\beta_2 \Pi_2) + \tau_2 \Delta t \partial_{t_2}^2 \phi + \tau_4 \Delta t^3 \sum_j D_{1j}^4 f_j^{(0)} = 0. \quad (24)$$

$$\begin{aligned} \sum_j D_{1j}^4 f_j^{(0)} &= \partial_{t_1}^4 \phi + 4\partial_{t_1}^3 \partial_{x_1} \Pi_1 + 6\partial_{t_1}^2 \partial_{x_1}^2 (\Pi_{20} + \beta_2 \Pi_2) + 4\partial_{t_1} \partial_{x_1}^3 (\Pi_{30} + \beta_3 \Pi_3) + \partial_{x_1}^4 (\Pi_{40} + \beta_4 \Pi_4) \\ &= 3\partial_{t_1}^3 \partial_{x_1} \Pi_1 + 6\partial_{t_1}^2 \partial_{x_1}^2 (\Pi_{20} + \beta_2 \Pi_2) + 4\partial_{t_1} \partial_{x_1}^3 (\Pi_{30} + \beta_3 \Pi_3) + \partial_{x_1}^4 (\Pi_{40} + \beta_4 \Pi_4) \\ &= \partial_{t_1}^2 \partial_{x_1}^2 (3\Pi_{20} + 6\beta_2 \Pi_2) + 4\partial_{t_1} \partial_{x_1}^3 (\Pi_{30} + \beta_3 \Pi_3) + \partial_{x_1}^4 (\Pi_{40} + \beta_4 \Pi_4) \\ &= \partial_{t_1}^2 \partial_{x_1}^2 \Pi_{20} + \partial_{t_1} \partial_{x_1}^3 (2\Pi_{30} + 4\beta_3 \Pi_3) + \partial_{x_1}^4 (\Pi_{40} + \beta_4 \Pi_4) \\ &= \partial_{x_1}^3 (\partial_{t_1} (2\Pi_{30} - \tilde{\Pi}_{30} + 4\beta_3 \Pi_3) + \partial_{x_1} \Pi_{40}) + \beta_4 \partial_{x_1}^4 \Pi_4, \end{aligned} \quad (25)$$

where $\tilde{\Pi}_{30}$ satisfies that $\partial_{t_1}\Pi_{20} + \partial_{x_1}\tilde{\Pi}_{30} = 0$, that is, $\tilde{\Pi}_{30} = \int \partial_\phi \Pi_{20} \partial_\phi \Pi_1 d\phi$.

If we take Π_{40} such that $\partial_{t_1}(2\Pi_{30} - \tilde{\Pi}_{30} + 4\beta_3\Pi_3) + \partial_{x_1}\Pi_{40} = 0$, that is,

$$\Pi_{40} = \int \partial_\phi (2\Pi_{30} - \tilde{\Pi}_{30} + 4\beta_3\Pi_3) \partial_\phi \Pi_1 d\phi = \int [(\partial_\phi \Pi_1)^4 + 6\beta_2 \partial_\phi \Pi_2 (\partial_\phi \Pi_1)^2 + 4\beta_3 \partial_\phi \Pi_3 \partial_\phi \Pi_1] d\phi, \quad (26)$$

then from Eqs. (24) and (25) we have

$$\partial_{t_4}\phi + 3\tau_3\beta_2\Delta t^2\partial_{t_2}\partial_{x_1}^2\Pi_2 + \tau_2\Delta t\partial_{t_2}^2\phi + \alpha_4\partial_{x_1}^4\Pi_4 = 0, \quad (27)$$

with $\alpha_4 = \Delta t^3\tau_4\beta_4$.

Note that there are two additional terms $3\tau_3\beta_2\Delta t^2\partial_{t_2}\partial_{x_1}^2\Pi_2$ and $\tau_2\Delta t\partial_{t_2}^2\phi$ in Eq. (27) should be removed when correctly recovering Eq. (1). From Eq. (18), we have

$$3\tau_3\beta_2\Delta t^2\partial_{t_2}\partial_{x_1}^2\Pi_2 + \tau_2\Delta t\partial_{t_2}^2\phi = (3\beta_2\tau_3\Delta t^2 - \alpha_2\tau_2\Delta t)\partial_{t_2}\partial_{x_1}^2\Pi_2 = (3\tau_3 - \tau_2^2)\beta_2\Delta t^2\partial_{t_2}\partial_{x_1}^2\Pi_2. \quad (28)$$

If $\Pi_2 = \phi$, then it follows from Eq. (18) that

$$3\tau_3\beta_2\Delta t^2\partial_{t_2}\partial_{x_1}^2\Pi_2 + \tau_2\Delta t\partial_{t_2}^2\phi = -\tau_2(3\tau_3 - \tau_2^2)\beta_2^2\Delta t^3\partial_{x_1}^4\phi. \quad (29)$$

Combining above expression and Eq. (25), we modify Π_{40} as

$$\Pi_{40} = \int [(\partial_\phi \Pi_1)^4 + 6\beta_2 \partial_\phi \Pi_2 (\partial_\phi \Pi_1)^2 + 4\beta_3 \partial_\phi \Pi_3 \partial_\phi \Pi_1 + A_{40}] d\phi, \quad (30)$$

where $A_{40} = \frac{\tau_2(3\tau_3 - \tau_2^2)\beta_2^2}{\tau_4}$, and Eq. (27) becomes

$$\partial_{t_4}\phi + \alpha_4\partial_{x_1}^4\Pi_4 = 0, \quad (31)$$

with $\alpha_4 = \Delta t^3\tau_4\beta_4$.

Therefore, when $\Pi_2 = \phi$, combining Eqs. (15), (18), (22) and (31), the fourth-order NPDE is exactly recovered to order $O(\epsilon^4)$

$$\partial_t\phi + \partial_x\Pi_1(\phi) + \alpha_2\partial_x^2\Pi_2(\phi) + \alpha_3\partial_x^3\Pi_3(\phi) + \alpha_4\partial_x^4\Pi_4(\phi) = 0, \quad (32)$$

with $\alpha_2 = \Delta t\tau_2\beta_2$, $\alpha_3 = \Delta t^2\tau_3\beta_3$, $\alpha_4 = \Delta t^3\tau_4\beta_4$.

Remark 2. If $\alpha_2 = 0$ or $\Pi_2 = 0$, then we take $\beta_2 = 0$ which leads to $A_{40}=0$. For this case, the modification of Π_{40} is not needed, and the fourth-order NPDE is exactly recovered.

Remark 3. The present model with a D1Q5 lattice can be used to simulate the fourth-order NPDEs with the form as Eq. (1) which contains some Kuramoto-Sivashinsky-type equations. Recently, following the idea in Ref. [20] two similar LBGK models with order $O(\epsilon^4)$ were given in Refs. [49] and [50], one for solving a class of three-order NPDEs which were first solved by the LBGK model in Ref. [20], and the other for the generalized Kuramoto-Sivashinsky equation. It can be easily found that the models in Refs. [49] and [50] do not satisfy the moments conditions (3) for $m = 4$. In fact, the so-called *amending-function* [49, 50] with order $O(\Delta t^2)$ implies that there is a stronger assumption on the nonlinear terms in EDF of the models. In addition, no comparisons were given to show the *higher-order* LBGK model in Ref. [49] superior to some lower-order LBGK models.

E. Recovery of the Fifth-Order NPDE

Summing Eq. (12) over j , and using Eqs. (3), (5), (15), (17), and (20), we obtain

$$\partial_{t_5}\phi + 3\tau_3\Delta t^2\partial_{t_3}\partial_{x_1}^2(\beta_2\Pi_2) + 2\tau_2\Delta t\partial_{t_2}\partial_{t_3}\phi + 4\tau_4\Delta t^3\partial_{t_2}\partial_{x_1}^3(\beta_3\Pi_3) + \tau_5\Delta t^4\sum_j D_{1j}^5 f_j^{(0)} = 0. \quad (33)$$

Using the similar procedure as Eq. (25), we can obtain

$$\sum_j D_{1j}^5 f_j^{(0)} = \beta_5\partial_{x_1}^5\Pi_5, \quad (34)$$

with

$$\Pi_{50} = \int [(\partial_\phi \Pi_1)^5 + 10\beta_2 \partial_\phi \Pi_2 (\partial_\phi \Pi_1)^3 + 10\beta_3 \partial_\phi \Pi_3 (\partial_\phi \Pi_1)^2 + 5\beta_4 \partial_\phi \Pi_4 \partial_\phi \Pi_1] d\phi, \quad (35)$$

and Eq. (33) becomes

$$\partial_{t_5} \phi + 3\tau_3 \beta_2 \Delta t^2 \partial_{t_3} \partial_{x_1}^2 \Pi_2 + 2\tau_2 \Delta t \partial_{t_2} \partial_{t_3} \phi + 4\tau_4 \beta_3 \Delta t^3 \partial_{t_2} \partial_{x_1}^3 \Pi_3 + \alpha_5 \partial_{x_1}^5 \Pi_5 = 0, \quad (36)$$

with $\alpha_5 = \Delta t^4 \tau_5 \beta_5$.

If $\Pi_2 = \Pi_3 = \phi$, we can modify Π_{50} as

$$\Pi_{50} = \int [(\partial_\phi \Pi_1)^5 + 10\beta_2 \partial_\phi \Pi_2 (\partial_\phi \Pi_1)^3 + 10\beta_3 \partial_\phi \Pi_3 (\partial_\phi \Pi_1)^2 + 5\beta_4 \partial_\phi \Pi_4 \partial_\phi \Pi_1 + A_{50}] d\phi, \quad (37)$$

where $A_{50} = \frac{(4\tau_2 \tau_4 + 3\tau_3^2 - 2\tau_2^2 \tau_3) \beta_2 \beta_3}{\tau_5}$, and Eq. (36) becomes

$$\partial_{t_5} \phi + \alpha_5 \partial_{x_1}^5 \Pi_5 = 0. \quad (38)$$

Combining Eqs. (15), (18), (22), (31) and (38), the fifth-order NPDE is exactly recovered to order $O(\epsilon^5)$

$$\partial_t \phi + \partial_x \Pi_1(\phi) + \sum_{k=2}^5 \alpha_k \partial_x^k \Pi_k(\phi) = 0, \quad (39)$$

with $\alpha_k = \Delta t^{k-1} \tau_k \beta_k$, $k = 2, \dots, 5$.

Remark 4. If $\alpha_2 = 0$ or $\alpha_3 = 0$, then $\beta_2 = 0$ or $\beta_3 = 0$ which leads to $A_{50} = 0$. For this case, the modification of Π_{50} is not needed, and the fifth-order NPDE is exactly recovered. The present model with a D1Q6 or D1Q7 lattice can be used to simulate the fifth-order NPDE (1) ($m = 5$) which contains some Kawahara-like equations.

F. Recovery of the Sixth-Order NPDE

Summing Eq. (13) over j , and using Eqs. (3), (5), (15), (17), (20), and (25), we obtain

$$\begin{aligned} \partial_{t_6} \phi + 3\tau_3 \Delta t^2 \partial_{t_4} \partial_{x_1}^2 (\beta_2 \Pi_2) + 2\tau_2 \Delta t \partial_{t_2} \partial_{t_4} \phi + 6\tau_4 \Delta t^3 \partial_{t_2}^2 \partial_{x_1}^2 (\beta_2 \Pi_2) + \tau_3 \Delta t^2 \partial_{t_2}^3 \phi + \tau_2 \Delta t \partial_{t_3}^2 \phi \\ + 4\tau_4 \Delta t^3 \partial_{t_3} \partial_{x_1}^3 (\beta_3 \Pi_3) + 5\tau_5 \Delta t^4 \partial_{t_2} \partial_{x_1}^4 (\beta_4 \Pi_4) + \tau_6 \Delta t^5 \sum_j D_{1j}^6 f_j^{(0)} = 0. \end{aligned} \quad (40)$$

Using the similar procedure as Eq. (25), we can obtain

$$\sum_j D_{1j}^6 f_j^{(0)} = \beta_6 \partial_{x_1}^6 \Pi_6, \quad (41)$$

with

$$\Pi_{60} = \int [(\partial_\phi \Pi_1)^6 + 15\beta_2 \partial_\phi \Pi_2 (\partial_\phi \Pi_1)^4 + 20\beta_3 \partial_\phi \Pi_3 (\partial_\phi \Pi_1)^3 + 15\beta_4 \partial_\phi \Pi_4 (\partial_\phi \Pi_1)^2 + 6\beta_5 \partial_\phi \Pi_5 \partial_\phi \Pi_1] d\phi, \quad (42)$$

and Eq. (40) becomes

$$\begin{aligned} \partial_{t_6} \phi + 3\tau_3 \beta_2 \Delta t^2 \partial_{t_4} \partial_{x_1}^2 \Pi_2 + 2\tau_2 \Delta t \partial_{t_2} \partial_{t_4} \phi + 6\tau_4 \beta_2 \Delta t^3 \partial_{t_2}^2 \partial_{x_1}^2 \Pi_2 + \tau_3 \Delta t^2 \partial_{t_2}^3 \phi + \tau_2 \Delta t \partial_{t_3}^2 \phi \\ + 4\tau_4 \beta_3 \Delta t^3 \partial_{t_3} \partial_{x_1}^3 \Pi_3 + 5\tau_5 \beta_4 \Delta t^4 \partial_{t_2} \partial_{x_1}^4 \Pi_4 + \alpha_6 \partial_{x_1}^6 \Pi_6 = 0, \end{aligned} \quad (43)$$

with $\alpha_6 = \Delta t^5 \tau_6 \beta_6$.

If $\Pi_2 = \Pi_3 = \Pi_4 = \phi$, we can modify Π_{60} as

$$\Pi_{60} = \int [(\partial_\phi \Pi_1)^6 + 15\beta_2 \partial_\phi \Pi_2 (\partial_\phi \Pi_1)^4 + 20\beta_3 \partial_\phi \Pi_3 (\partial_\phi \Pi_1)^3 + 15\beta_4 \partial_\phi \Pi_4 (\partial_\phi \Pi_1)^2 + 6\beta_5 \partial_\phi \Pi_5 \partial_\phi \Pi_1 + A_{60}] d\phi, \quad (44)$$

where $A_{60} = \frac{(5\tau_2\tau_5+3\tau_3\tau_4-2\tau_2^2\tau_4)\beta_2\beta_4+(4\tau_4-\tau_2\tau_3)\tau_3\beta_3^2+(\tau_2\tau_3-6\tau_4)\tau_2^2\beta_2^3}{\tau_6}$, and Eq. (43) becomes

$$\partial_{t_6}\phi + \alpha_6\partial_{x_1}^6\Pi_6 = 0. \quad (45)$$

Combining Eqs. (15), (18), (22), (31), (38), and (45) the sixth-order NPDE is exactly recovered to order $O(\epsilon^6)$

$$\partial_t\phi + \partial_x\Pi_1(\phi) + \sum_{k=2}^6\alpha_k\partial_x^k\Pi_k(\phi) = 0, \quad (46)$$

with $\alpha_k = \Delta t^{k-1}\tau_k\beta_k$, $k = 2, \dots, 6$.

Remark 5. If $\alpha_2 = 0$ and $\Pi_3 = \phi$, then the sixth-order NPDE is exactly recovered. The present model with a D1Q7 lattice can be used to simulate six-order NPDE (1) ($m = 6$) which also contains some Kawahara-like equations.

III. EQUILIBRIUM DISTRIBUTION FUNCTIONS AND AUXILIARY MOMENTS

For a given NPDE of order m , Π_{k0} can be obtained from the related formula in above section ($2 \leq k \leq m$), and the number of discrete velocity directions is at least equal to $m + 1$. So we can use a D1Q5 LBGK model to solve the NPDE of order less than or equal to 4, and a D1Q7 one to solve the NPDE of order less than or equal to 6. A D1Q4 or D1Q6 one without the rest velocity can also be used to the NPDE of order 3 or 5. In this section we give only the EDFs and AMs for the LBGK models with D1Q5 and D1Q7 lattice, respectively.

A. Equilibrium Distribution Functions for LBGK Model with D1Q5 Lattice

Denoting $\bar{\Pi}_0 = \phi$, $\bar{\Pi}_1 = \Pi_1/c$, $\bar{\Pi}_k = (\Pi_{k0} + \beta_k\Pi_k)/c^k$, $k = 2, 3, 4$, the moments conditions (3) for $m = 4$ are rewritten as

$$\sum_j e_j^k f_j^{\text{eq}} = \bar{\Pi}_k, k = 0, \dots, 4 \quad (47)$$

where $\{e_0, e_1, e_2, e_3, e_4\} = \{0, 1, -1, 2, -2\}$. Let

$$\vec{\Pi} = [\bar{\Pi}_0, \bar{\Pi}_1, \dots, \bar{\Pi}_4]^T, \vec{f}^{\text{eq}} = [f_0^{\text{eq}}, f_1^{\text{eq}}, \dots, f_4^{\text{eq}}]^T. \quad (48)$$

From Eq. (47), we have

$$\mathbf{M}_5 \vec{f}^{\text{eq}} = \vec{\Pi}, \quad (49)$$

where

$$\mathbf{M}_5 = \begin{bmatrix} 1 & 1 & 1 & 1 & 1 \\ 0 & 1 & -1 & 2 & -2 \\ 0 & 1 & 1 & 4 & 4 \\ 0 & 1 & -1 & 8 & -8 \\ 0 & 1 & 1 & 16 & 16 \end{bmatrix},$$

It is easy to find the inverse of \mathbf{M}_5

$$\mathbf{M}_5^{-1} = \frac{1}{24} \begin{bmatrix} 24 & 0 & -30 & 0 & 6 \\ 0 & 16 & 16 & -4 & -4 \\ 0 & -16 & 16 & 4 & -4 \\ 0 & -2 & -1 & 2 & 1 \\ 0 & 2 & -1 & -2 & 1 \end{bmatrix},$$

thus

$$\vec{f}^{\text{eq}} = \mathbf{M}_5^{-1} \vec{\Pi}. \quad (50)$$

Therefore, the EDFs of the LBGK model with D1Q5 lattice can be obtained as follows

$$\begin{aligned} f_0^{\text{eq}} &= [4\phi - 5\bar{\Pi}_2 + \bar{\Pi}_4] / 4, \\ f_1^{\text{eq}} &= [4(\bar{\Pi}_1 + \bar{\Pi}_2) - \bar{\Pi}_3 - \bar{\Pi}_4] / 6, \\ f_2^{\text{eq}} &= [4(-\bar{\Pi}_1 + \bar{\Pi}_2) + \bar{\Pi}_3 - \bar{\Pi}_4] / 6, \\ f_3^{\text{eq}} &= [-2(\bar{\Pi}_1 - \bar{\Pi}_3) - \bar{\Pi}_2 + \bar{\Pi}_4] / 24, \\ f_4^{\text{eq}} &= [2(\bar{\Pi}_1 - \bar{\Pi}_3) - \bar{\Pi}_2 + \bar{\Pi}_4] / 24, \end{aligned} \quad (51)$$

B. Equilibrium Distribution Functions for LBGK with D1Q7 Lattice

Similarly, denoting $\bar{\Pi}_0 = \phi$, $\bar{\Pi}_1 = \Pi_1/c$, $\bar{\Pi}_k = (\Pi_{k0} + \beta_k \Pi_k)/c^k$, $k = 2, \dots, 6$, the moments conditions (3) for $m = 6$ are rewritten as

$$\sum_j e_j^k f_j^{\text{eq}} = \bar{\Pi}_k, k = 0, \dots, 6 \quad (52)$$

where $\{e_0, e_1, e_2, e_3, e_4, e_5, e_6\} = \{0, 1, -1, 2, -2, 3, -3\}$. Let

$$\vec{\Pi} = [\bar{\Pi}_0, \bar{\Pi}_1, \dots, \bar{\Pi}_6]^T, \vec{f}^{\text{eq}} = [f_0^{\text{eq}}, f_1^{\text{eq}}, \dots, f_6^{\text{eq}}]^T. \quad (53)$$

From Eq. (52), we have

$$\mathbf{M}_7 \vec{f}^{\text{eq}} = \vec{\Pi}, \quad (54)$$

where

$$\mathbf{M}_7 = \begin{bmatrix} 1 & 1 & 1 & 1 & 1 & 1 & 1 \\ 0 & 1 & -1 & 2 & -2 & 3 & -3 \\ 0 & 1 & 1 & 4 & 4 & 9 & 9 \\ 0 & 1 & -1 & 8 & -8 & 27 & -27 \\ 0 & 1 & 1 & 16 & 16 & 81 & 81 \\ 0 & 1 & -1 & 32 & -32 & 243 & -243 \\ 0 & 1 & 1 & 64 & 64 & 729 & 729 \end{bmatrix},$$

It is easy to find the inverse of \mathbf{M}_7

$$\mathbf{M}_7^{-1} = \frac{1}{720} \begin{bmatrix} 720 & 0 & -980 & 0 & 280 & 0 & -20 \\ 0 & 540 & 540 & -195 & -195 & 15 & 15 \\ 0 & -540 & 540 & 195 & -195 & -15 & 15 \\ 0 & -108 & -54 & 120 & 60 & -12 & -6 \\ 0 & 108 & -54 & -120 & 60 & 12 & -6 \\ 0 & 12 & 4 & -15 & -5 & 3 & 1 \\ 0 & -12 & 4 & 15 & -5 & -3 & 1 \end{bmatrix},$$

thus

$$\vec{f}^{\text{eq}} = \mathbf{M}_7^{-1} \vec{\Pi}. \quad (55)$$

Therefore, the EDFs of the LBGK model with D1Q7 lattice can be obtained as follows

$$\begin{aligned} f_0^{\text{eq}} &= [36\phi - 49\bar{\Pi}_2 + 14\bar{\Pi}_4 - \bar{\Pi}_6] / 36, \\ f_1^{\text{eq}} &= [36(\bar{\Pi}_1 + \bar{\Pi}_2) - 13(\bar{\Pi}_3 + \bar{\Pi}_4) + \bar{\Pi}_5 + \bar{\Pi}_6] / 48, \\ f_2^{\text{eq}} &= [36(-\bar{\Pi}_1 + \bar{\Pi}_2) + 13(\bar{\Pi}_3 - \bar{\Pi}_4) - \bar{\Pi}_5 + \bar{\Pi}_6] / 48, \\ f_3^{\text{eq}} &= [-18\bar{\Pi}_1 - 9\bar{\Pi}_2 + 20\bar{\Pi}_3 + 10\bar{\Pi}_4 - 2\bar{\Pi}_5 - \bar{\Pi}_6] / 120, \\ f_4^{\text{eq}} &= [18\bar{\Pi}_1 - 9\bar{\Pi}_2 - 20\bar{\Pi}_3 + 10\bar{\Pi}_4 + 2\bar{\Pi}_5 - \bar{\Pi}_6] / 120, \\ f_5^{\text{eq}} &= [12\bar{\Pi}_1 + 4\bar{\Pi}_2 - 15\bar{\Pi}_3 - 5\bar{\Pi}_4 + 3\bar{\Pi}_5 + \bar{\Pi}_6] / 720, \\ f_6^{\text{eq}} &= [-12\bar{\Pi}_1 + 4\bar{\Pi}_2 + 15\bar{\Pi}_3 - 5\bar{\Pi}_4 - 3\bar{\Pi}_5 + \bar{\Pi}_6] / 720, \end{aligned} \quad (56)$$

C. Auxiliary Moments

For a given NPDE of order m , $\Pi_k(1 \leq k \leq m)$ are known, and $\Pi_{k0}(2 \leq k \leq m)$ can be obtained by using the formula in Sec. II., then we can obtain the EDFs of related LBGK model with suitable lattice, and the LBGK model is derived. For example, the EDFs of D1Q5 or D1Q7 LBGK model can be computed by Eq. (51), or Eq. (56). In simulations in the present work, two classes of concrete NPDEs are considered, and the related AMs of these NPDEs are given below.

(1) Sixth-order NPDEs

$$u_t + \alpha u u_x + \beta u^n u_x + \sum_{k=2}^6 \alpha_k \partial_x^k u = 0, \quad (57)$$

where α, β, n and $\alpha_k(2 \leq k \leq 6)$ are constants, and $n \geq 0$. Equation (57) contains many well-known equations, such as the KdV-Burgers equation, (m)KdV equation, Kuramoto-Sivashinsky equation, Kawahara equation, and some of their extensions.

We can use a LBGK model with D1Q7 lattice to solve Eq. (57), and the first seven moments are needed. Since $\Pi_1 = \frac{\alpha}{2}u^2 + \frac{\beta}{n+1}u^{n+1}$, $\Pi_k = u, k \geq 2$, we have $\Pi'_1 = \alpha u + \beta u^n, \Pi'_k = 1, k \geq 2$. Equation (57) can be exactly recovered by using the LBGK model proposed above, and the exact expressions of AM functions $\Pi_{k0}(2 \leq k \leq 6)$ can be obtained as follows by using the formula in Sec. II.

$$\begin{aligned} \Pi_{20} &= \int (\Pi'_1)^2 du, \\ \Pi_{30} &= \int [(\Pi'_1)^3 + 3\beta_2 \Pi'_2 \Pi'_1] du = \int (\Pi'_1)^3 du + 3\beta_2 \Pi_1, \\ \Pi_{40} &= \int [(\Pi'_1)^4 + 6\beta_2 \Pi'_2 (\Pi'_1)^2 + 4\beta_3 \Pi'_3 \Pi'_1 + A_{40}] du = \int (\Pi'_1)^4 du + 6\beta_2 \Pi_{20} + 4\beta_3 \Pi_1 + A_{40}u, \\ \Pi_{50} &= \int [(\Pi'_1)^5 + 10\beta_2 \Pi'_2 (\Pi'_1)^3 + 10\beta_3 \Pi'_3 (\Pi'_1)^2 + 5\beta_4 \Pi'_4 \Pi'_1 + A_{50}] du \\ &= \int [(\Pi'_1)^5 + 10\beta_2 (\Pi'_1)^3] du + 10\beta_3 \Pi_{20} + 5\beta_4 \Pi_1 + A_{50}u, \\ \Pi_{60} &= \int [(\Pi'_1)^6 + 15\beta_2 \Pi'_2 (\Pi'_1)^4 + 20\beta_3 \Pi'_3 (\Pi'_1)^3 + 15\beta_4 \Pi'_4 (\Pi'_1)^2 + 6\beta_5 \Pi'_5 \Pi'_1 + A_{60}] du \\ &= \int [(\Pi'_1)^6 + 15\beta_2 (\Pi'_1)^4 + 20\beta_3 (\Pi'_1)^3] du + 15\beta_4 \Pi_{20} + 6\beta_5 \Pi_1 + A_{60}u, \end{aligned} \quad (58)$$

where

$$\begin{aligned} \alpha_k &= \Delta t^{k-1} \tau_k \beta_k, 2 \leq k \leq 6, \\ A_{40} &= \frac{\tau_2(3\tau_3 - \tau_2^2)\beta_2^2}{\tau_4}, \\ A_{50} &= \frac{(4\tau_2\tau_4 + 3\tau_3^2 - 2\tau_2^2\tau_3)\beta_2\beta_3}{\tau_5}, \\ A_{60} &= \frac{(5\tau_2\tau_5 + 3\tau_3\tau_4 - 2\tau_2^2\tau_4)\beta_2\beta_4 + (4\tau_4 - \tau_2\tau_3)\tau_3\beta_3^2 + (\tau_2\tau_3 - 6\tau_4)\tau_2^2\beta_2^3}{\tau_6}, \end{aligned} \quad (59)$$

and it is easily obtained that

$$\int (\Pi'_1)^k du = \sum_{j=0}^k \int C_k^j (\alpha u)^{k-j} (\beta u^n)^j du = u \left[\sum_{j=0}^k \frac{1}{jn + k + 1 - j} C_k^j (\alpha u)^{k-j} (\beta u^n)^j \right], 2 \leq k \leq 6. \quad (60)$$

For $k = 2, 3, 4$ we have

$$\begin{aligned}\int (\Pi_1')^2 du &= u \left[\frac{1}{3}(\alpha u)^2 + \frac{2}{n+2}(\alpha u)(\beta u^n) + \frac{1}{2n+1}(\beta u^n)^2 \right], \\ \int (\Pi_1')^3 du &= u \left[\frac{1}{4}(\alpha u)^3 + \frac{3}{n+3}(\alpha u)^2(\beta u^n) + \frac{3}{2n+2}(\alpha u)(\beta u^n)^2 + \frac{1}{3n+1}(\beta u^n)^3 \right], \\ \int (\Pi_1')^4 du &= u \left[\frac{1}{5}(\alpha u)^4 + \frac{4}{n+4}(\alpha u)^3(\beta u^n) + \frac{6}{2n+3}(\alpha u)^2(\beta u^n)^2 + \frac{4}{3n+2}(\alpha u)(\beta u^n)^3 + \frac{1}{4n+1}(\beta u^n)^4 \right].\end{aligned}\quad (61)$$

(2) Third-order NPDEs

$$u_t + \alpha u u_x + \beta u^n u_x + \alpha_2 (u^p)_{xx} + \alpha_3 (u^q)_{xxx} = 0, \quad (62)$$

where $\alpha, \beta, \alpha_2, \alpha_3, n, p$ and q are constants, and $n \geq 0, p \geq 1$, and $q \geq 1$. Eq. (62) contains also many well-known equations, such as the KdV-Burgers equation, (m)KdV equation, and $\bar{K}(p, q)$ equation.

We can use a LBGK model with D1Q4 or D1Q5 lattice to solve Eq. (62), and if the C-E expansion to order $O(\epsilon^3)$ is used, we need only to give the first four moments, while for the C-E expansion to order $O(\epsilon^4)$, the first five moments are needed. Since $\Pi_1 = \frac{\alpha}{2}u^2 + \frac{\beta}{n+1}u^{n+1}$, $\Pi_2 = u^p$ and $\Pi_3 = u^q$, we can exactly recover Eq. (62) by using the LBGK model proposed above, and the exact expressions of AM functions Π_{20} , Π_{30} and Π_{40} can be obtained as follows by using the formula in Sec. II.

$$\begin{aligned}\Pi_{20} &= \int (\Pi_1')^2 du, \\ \Pi_{30} &= \int [(\Pi_1')^3 + 3\beta_2 \Pi_2' \Pi_1'] du = \int [(\Pi_1')^3 + 3\beta_2 p u^{p-1}(\alpha u + \beta u^n)] du \\ &= \int (\Pi_1')^3 du + 3\beta_2 p u^p \left[\frac{\alpha u}{p+1} + \frac{\beta u^n}{p+n} \right], \\ \Pi_{40} &= \int [(\Pi_1')^4 + 6\beta_2 \Pi_2' (\Pi_1')^2 + 4\beta_3 \Pi_3' \Pi_1' + A_{40}] du \\ &= \int (\Pi_1')^4 du + 6\beta_2 p u^p \left[\frac{(\alpha u)^2}{p+2} + \frac{2(\alpha u)(\beta u^n)}{p+n+1} + \frac{(\beta u^n)^2}{p+2n} \right] + 4\beta_3 q u^q \left[\frac{\alpha u}{q+1} + \frac{\beta u^n}{q+n} \right] + A_{40} u,\end{aligned}\quad (63)$$

where A_{40} , $\int (\Pi_1')^2 du$, $\int (\Pi_1')^3 du$, and $\int (\Pi_1')^4 du$ can be computed by Eqs. (59) and (61).

IV. SIMULATION RESULTS

To test the LBGK model proposed above, three classes of NPDEs with exact solutions are simulated, including four Kuramoto-Sivashinsky-like equations, three Kawahara-like equations and two KdV-like equations. In all simulations, if not specified, we use the nonequilibrium extrapolation scheme proposed by Guo *et al.* [51] to treat the exact boundary condition, and the initial and boundary conditions of the test problems with analytical solutions are determined by their analytical solutions. The D1Q5 and D1Q7 LBGK models are used to simulate the test problems. The following global relative error is used to measure the accuracy:

$$E = \frac{\sum_j |\phi(\mathbf{x}_j, t) - \phi^*(\mathbf{x}_j, t)|}{\sum_j |\phi^*(\mathbf{x}_j, t)|}, \quad (64)$$

where ϕ and ϕ^* are the numerical solution and analytical one, respectively, and the summation is taken over all grid points.

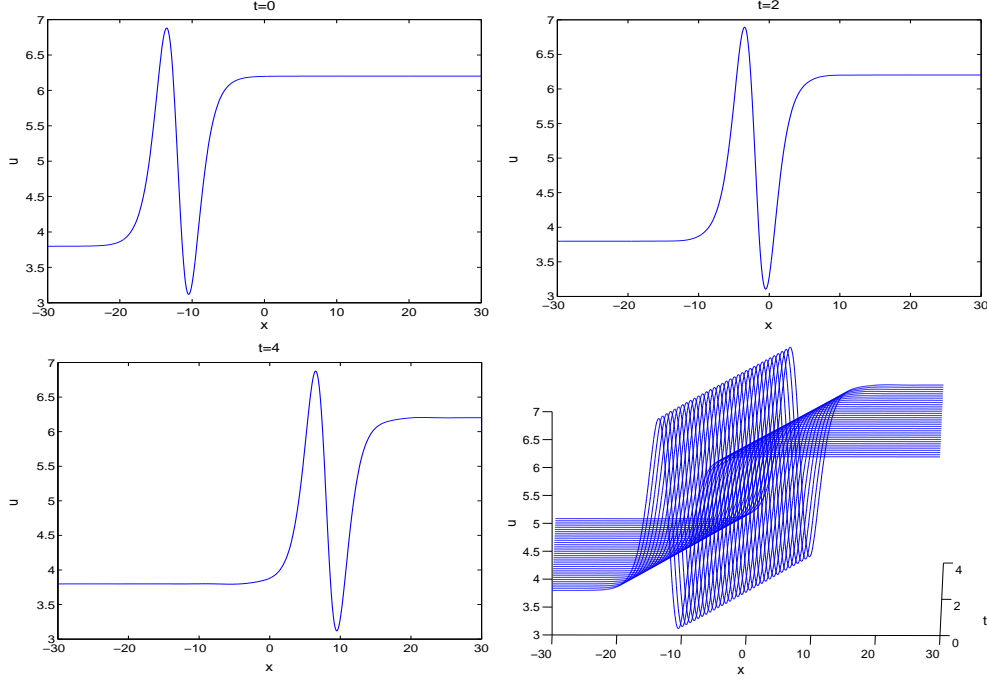
The first four test problems are the fourth-order Kuramoto-Sivashinsky-type equations, and three of them were simulated by the LBGK model in Ref. [50]. We use the D1Q5 LBGK model to simulate them and compare the proposed model with that in Ref. [50].

Example 4.1. The Kuramoto-Sivashinsky equation [42]

$$u_t + uu_x + u_{xx} + u_{xxxx} = 0, \quad (65)$$

TABLE I: Comparison of global relative errors at different times [(1) $t = 1$; (2) $t = 2$; (3) $t = 3$; (4) $t = 4$].

(c, τ_{opt})	Present Model			Model in Ref. [50]		
	(10, 5.99)	(100, 1.989)	(1000, 1.27)	(10, 3.346)	(100, 1.998)	(1000, 1.2705)
(1)	9.6476×10^{-3}	2.9926×10^{-3}	6.0570×10^{-4}	2.6571×10^{-2}	3.2655×10^{-3}	6.5581×10^{-4}
(2)	1.2962×10^{-2}	4.2992×10^{-3}	8.7427×10^{-4}	3.7065×10^{-2}	5.3215×10^{-3}	1.1121×10^{-3}
(3)	1.7247×10^{-2}	5.5078×10^{-3}	1.1185×10^{-3}	5.0615×10^{-2}	7.1611×10^{-3}	1.5426×10^{-3}
(4)	2.2122×10^{-2}	6.8650×10^{-3}	1.3738×10^{-3}	8.0887×10^{-2}	8.9284×10^{-3}	1.9441×10^{-3}

FIG. 1: (Color online) The shock profile wave propagation of the KS equation (65), $b = 5, k = \frac{1}{2}\sqrt{\frac{11}{19}}, x_0 = -12$. Exact boundary condition in $[-30, 30]$, $\Delta x = 0.1, \Delta t = 0.0001$.

with the exact solution

$$u(x, t) = b + \frac{15}{19} \sqrt{\frac{11}{19}} \left(-9 \tanh(k(x - bt - x_0)) + 11 \tanh^3(k(x - bt - x_0)) \right), \quad (66)$$

where b, k, x_0 are parameters.

In simulations, we set $b = 5, k = \frac{1}{2}\sqrt{\frac{11}{19}}$, and $x_0 = -12$ as in Ref. [50] for comparison. The simulation is conducted in $[-30, 30]$ with $\Delta x = 0.1, \Delta t = 0.01, 0.001$, and 0.0001 , corresponding to $c = 10, 100$, and 1000 , respectively. The errors are listed in Table I for different times, where τ_{opt} is the optimal one corresponding to the minimal error. We also present the regular shock profile wave propagation for Eq. (65) with Eq. (66) in Fig. 1. From the table it can be seen that the errors of our model are smaller than those of the model in Ref. [50], and the accuracy of our model for $\Delta t = 0.01$ is much better than that of the model in Ref. [50]. When Δt is small enough, the effect of truncated errors of the model in Ref. [50] can be ignored, thus the difference between the present model and that in Ref. [50] is less.

Example 4.2. The Kuramoto-Sivashinsky equation [42]

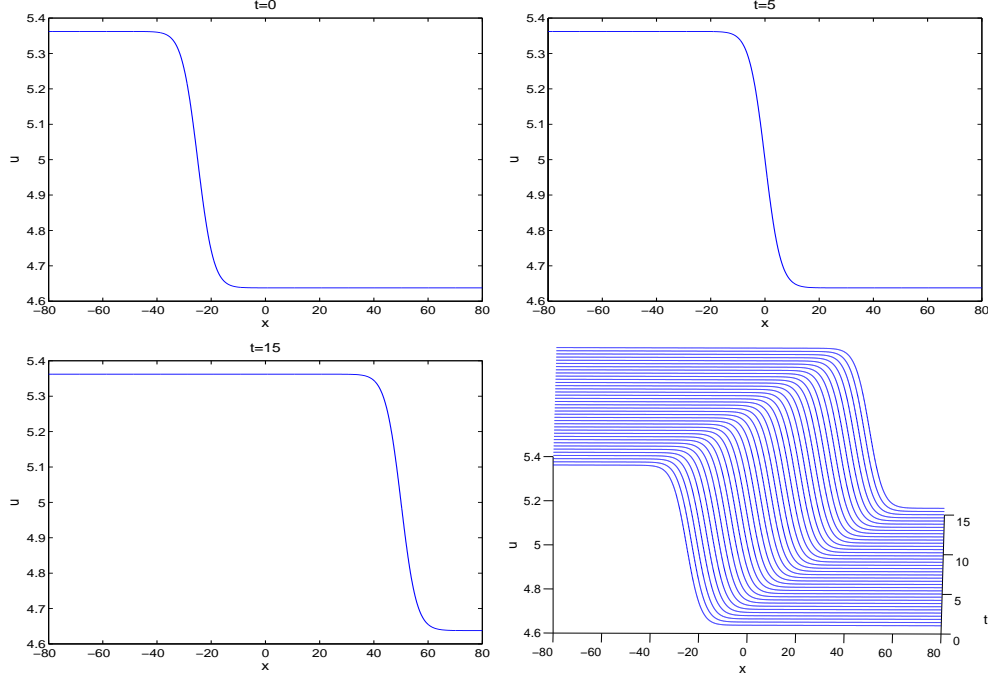
$$u_t + uu_x - u_{xx} + u_{xxx} = 0, \quad (67)$$

with the exact solution

$$u(x, t) = b + \frac{15}{19\sqrt{19}} \left(-3 \tanh(k(x - bt - x_0)) + \tanh^3(k(x - bt - x_0)) \right), \quad (68)$$

TABLE II: Comparison of global relative errors at different times [(1) $t = 6$; (2) $t = 8$; (3) $t = 10$; (4) $t = 12$].

(c, τ_{opt})	Present Model			Model in Ref. [50]		
	(10, 4.569)	(100, 2.076)	(1000, 1.277)	(10, 4.0)	(100, 2.063)	(1000, 1.277)
(1)	2.8486×10^{-5}	1.5343×10^{-6}	2.7448×10^{-7}	1.2313×10^{-3}	5.6085×10^{-5}	7.6750×10^{-6}
(2)	3.1775×10^{-5}	1.6534×10^{-6}	2.9535×10^{-7}	1.5818×10^{-3}	6.9643×10^{-5}	9.3058×10^{-6}
(3)	3.3937×10^{-5}	1.7189×10^{-6}	3.0741×10^{-7}	1.9018×10^{-3}	8.1373×10^{-5}	1.0640×10^{-5}
(4)	3.4934×10^{-5}	1.8264×10^{-6}	4.2625×10^{-7}	2.1886×10^{-3}	9.1494×10^{-5}	1.1661×10^{-5}

FIG. 2: (Color online) The shock profile wave propagation of the KS equation (67), $b = 5$, $k = \frac{1}{2\sqrt{19}}$, $x_0 = -25$. Exact boundary condition in $[-80, 80]$, $\Delta x = 0.1$, $\Delta t = 0.01$.

where b, k, x_0 are parameters.

In simulations, we set $b = 5$, $k = \frac{1}{2\sqrt{19}}$, and $x_0 = -25$ as in Ref. [50] for comparison. The simulation is conducted in $[-50, 50]$ with $\Delta x = 0.1$, $\Delta t = 0.001$ and 0.0001 . The errors are listed in Table II. for different times, and the regular shock profile wave propagation for Eq. (67) is shown in Fig. 2. From the table it can be seen that the errors of our model are much smaller than those of the model in Ref. [50].

Example 4.3. The generalized Kuramoto-Sivashinsky equation [42]

$$u_t + uu_x + u_{xx} + \sigma u_{xxx} + u_{xxxx} = 0, \quad (69)$$

with the exact solution

$$u(x, t) = b + 9 - 15 \left(\tanh(k(x - bt - x_0)) + \tanh^2(k(x - bt - x_0)) - \tanh^3(k(x - bt - x_0)) \right), \quad (70)$$

where σ, b, k, x_0 are parameters.

In simulations, we set $\sigma = 4$, $b = 6$, $k = \frac{1}{2}$, and $x_0 = -10$ as in Ref. [50] for comparison. The simulation is performed in $[-30, 30]$ with $\Delta x = 0.1$, $\Delta t = 0.01, 0.001$ and 0.0001 . Table III gives the errors of numerical solution at different times. We also present the solitary wave propagation for Eq. (69) is shown in Fig. 3. From the table it can be seen that the errors of our model for the smallest Δt are larger than those of the model in Ref. [50], while the accuracy and stability of the present model for larger Δt are better than those of the model in Ref. [50]. It is noted that the accuracy of both models for Eq. (69) is much larger than for Eqs. (65) and (67).

Example 4.4. The generalized Kuramoto-Sivashinsky equation [52]

$$u_t + 3u^3u_x + au_{xx} - bu_{xxx} + u_{xxxx} = 0, \quad (71)$$

TABLE III: Comparison of global relative errors at different times [(1) $t = 1$; (2) $t = 2$; (3) $t = 3$; (4) $t = 4$; '-' means that the scheme is divergent].

(c, τ_{opt})	Present Model			Model in Ref. [50]		
	(10, 7.082)	(100, 9.89)	(1000, 1.267)	(10, 3.47)	(100, 1.975)	(1000, 1.267486)
(1)	4.1701×10^{-1}	5.2017×10^{-2}	5.1020×10^{-2}	9.7859×10^{-1}	1.3802×10^{-1}	2.6054×10^{-2}
(2)	1.2376×10^{-0}	6.9440×10^{-2}	5.6700×10^{-2}	-	1.4077×10^{-1}	2.8329×10^{-2}
(3)	2.5757×10^{-0}	9.7967×10^{-2}	5.1337×10^{-2}	-	1.7050×10^{-1}	2.6802×10^{-2}
(4)	3.4682×10^{-0}	1.6776×10^{-1}	6.5639×10^{-2}	-	3.1488×10^{-1}	3.5225×10^{-2}

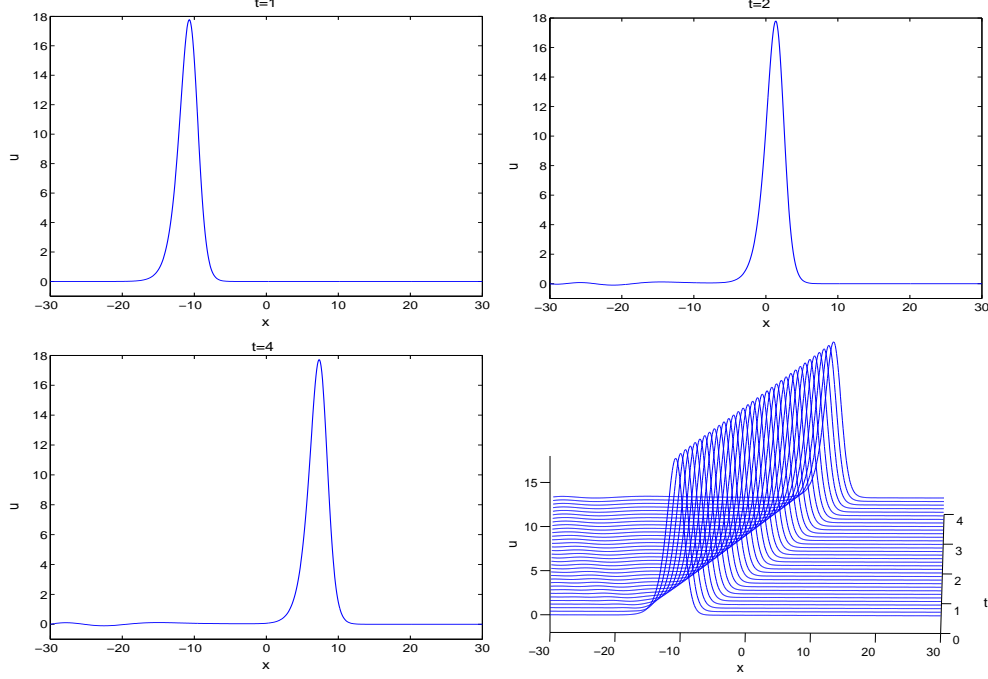


FIG. 3: (Color online) The solitary wave propagation of the GKS equation (69), $b = 6, \sigma = 4, k = \frac{1}{2}, x_0 = -10$. Exact boundary condition in $[-30, 30]$, $\Delta x = 0.1, \Delta t = 0.0001$.

with the exact solution

$$u(x, t) = \frac{\sqrt{3}b}{2\sqrt{2}} \tanh \left[\frac{\sqrt{3}b}{4\sqrt{2}} \left(x - x_0 - \frac{29b^3}{144}t \right) + \frac{C}{2} \right] + \frac{b}{6}, \quad (72)$$

where a, b, C are constants.

In simulations, we set $a = 1, b = 1$, and $C = 1$. The simulation is performed in $[-30, 30]$ with $x_0 = 0, \Delta x = 0.1, \Delta t = 0.01, 0.001$ and 0.0001 , and both D1Q5 and D1Q7 LBGK models are used. Table IV gives the errors of numerical solution at different times, and the regular shock profile wave propagation for Eq. (71) is shown in Fig. 4. From the table It found that the numerical solutions are agree well with the analytic ones, and the accuracy of D1q7 model is much better than that of D1Q5 one for smaller Δt .

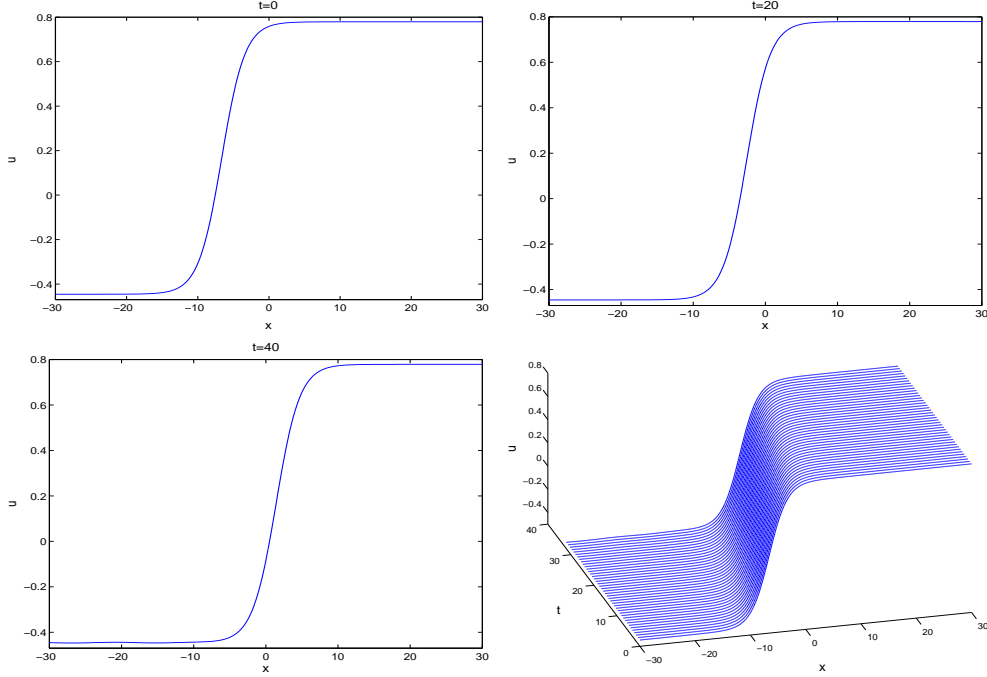
The next three test problems are the fifth-order Kawahara-like equations. We use the D1Q7 LBGK model to simulate them. Since the first six constraints on moments are enough for exactly recovering the fifth-order NPDEs in C-E expansion, it is interesting to compare the present *exact* model with C-E expansion to order $O(\epsilon^6)$ with one to order $O(\epsilon^5)$. We denote scheme 1 and scheme 2 for the model of order $O(\epsilon^6)$ and that of order $O(\epsilon^5)$, respectively. For simplification, we only take $\bar{\Pi}_6 = 0$ in Eq. (56) for scheme 2 in simulations.

Example 4.5. The Kawahara equation [53]

$$u_t + \alpha uu_x + \beta u_{xxx} + \gamma u_{xxxxx} = 0, \quad (73)$$

TABLE IV: Comparison of global relative errors at different times [(1) $t = 1$; (2) $t = 2$; (3) $t = 3$; (4) $t = 4$].

(c, τ_{opt})	D1Q5 Model			D1Q7 Model		
	(10, 3.32)	(100, 2.0)	(1000, 1.27)	(10, 4.14)	(100, 2.31)	(1000, 1.40)
(1)	1.4921×10^{-3}	3.7819×10^{-4}	7.5629×10^{-5}	1.3234×10^{-3}	8.7735×10^{-5}	4.2032×10^{-6}
(2)	3.1612×10^{-3}	7.8311×10^{-4}	1.5509×10^{-4}	2.6053×10^{-3}	1.5272×10^{-4}	6.9690×10^{-6}
(3)	5.0988×10^{-3}	1.2215×10^{-3}	2.4006×10^{-4}	4.1570×10^{-3}	2.2473×10^{-4}	1.0021×10^{-5}
(4)	7.2939×10^{-3}	1.6930×10^{-3}	3.3080×10^{-4}	6.0013×10^{-3}	3.0868×10^{-4}	1.3604×10^{-5}

FIG. 4: (Color online) The shock profile wave propagation of the GKS equation (71), $a = b = C = 1, x_0 = -5$. Exact boundary condition in $[-30, 30]$, $\Delta x = 0.1, \Delta t = 0.0001$.

with the exact solution

$$u(x, t) = A \operatorname{sech}^4[B(x - Ct)], \quad (74)$$

where α, β, γ are constants, and $A = -\frac{105\beta^2}{169\alpha\gamma}, B = \frac{1}{2}\sqrt{-\frac{\beta}{13\gamma}}, C = -\frac{36\beta^2}{169\gamma}$.

In simulations, we set $\alpha = \beta = -\gamma = 1$. The simulation is conducted in $[-30, 30]$ with $\Delta x = 0.1, \Delta t = 0.01, 0.001$ and 0.0001 . Table V. gives the errors of numerical solution for different times. From the table it is found that there is little difference between accuracy of two schemes, which implies that the accuracy of higher-order model may not be better than that of lower-order one.

TABLE V: Comparison of global relative errors at different times [(1) $t = 1$, (2) $t = 2$; (3) $t = 3$; (4) $t = 4$].

(c, τ_{opt})	Scheme 1			Scheme 2		
	(10, 3.37)	(100, 2.53)	(1000, 2.02)	(10, 3.35)	(100, 2.55)	(1000, 2.04)
(1)	6.0101×10^{-3}	2.6928×10^{-3}	1.5361×10^{-3}	5.9364×10^{-3}	2.7372×10^{-3}	1.5750×10^{-3}
(2)	1.0877×10^{-2}	5.2590×10^{-3}	3.0032×10^{-3}	1.0698×10^{-2}	5.3477×10^{-3}	3.0827×10^{-3}
(3)	1.5605×10^{-2}	7.5403×10^{-3}	4.2350×10^{-3}	1.5369×10^{-2}	7.6869×10^{-3}	4.3599×10^{-3}
(4)	2.0197×10^{-2}	9.4960×10^{-3}	5.3288×10^{-3}	2.0035×10^{-2}	9.7447×10^{-3}	5.4829×10^{-3}

TABLE VI: Comparison of global relative errors at different times [(1) $t = 1$; (2) $t = 2$; (3) $t = 3$; (4) $t = 4$].

(c, τ_{opt})	Scheme 1			Scheme 2		
	(10, 4.54)	(100, 2.53)	(1000, 2.04)	(10, 4.04)	(100, 2.56)	(1000, 2.04)
(1)	1.9295×10^{-2}	7.1698×10^{-3}	4.4255×10^{-3}	1.6850×10^{-2}	7.3109×10^{-3}	4.4254×10^{-3}
(2)	3.8260×10^{-2}	1.3214×10^{-2}	7.7342×10^{-3}	3.2649×10^{-2}	1.3549×10^{-2}	7.7745×10^{-3}
(3)	5.7488×10^{-2}	1.7575×10^{-2}	1.0046×10^{-2}	4.7022×10^{-2}	1.8137×10^{-2}	1.0211×10^{-2}
(4)	7.4409×10^{-2}	2.1032×10^{-2}	1.1886×10^{-2}	6.0945×10^{-2}	2.2855×10^{-2}	1.2424×10^{-2}

TABLE VII: Comparison of global relative errors at different times [(1) $t = 1$; (2) $t = 2$; (3) $t = 3$; (4) $t = 4$].

(c, τ_{opt})	Scheme 1			Scheme 2		
	(10, 5.01)	(100, 3.31)	(1000, 2.28)	(10, 4.64)	(100, 2.95)	(1000, 2.18)
(1)	9.8169×10^{-3}	4.6248×10^{-3}	2.0662×10^{-3}	9.0008×10^{-3}	3.6976×10^{-3}	1.8557×10^{-3}
(2)	1.8335×10^{-2}	8.9484×10^{-3}	4.0584×10^{-3}	1.6575×10^{-2}	7.1666×10^{-3}	3.6371×10^{-3}
(3)	2.6841×10^{-2}	1.3201×10^{-2}	6.1428×10^{-3}	2.3973×10^{-2}	1.0468×10^{-2}	5.2117×10^{-3}
(4)	3.5872×10^{-2}	1.8257×10^{-2}	7.9304×10^{-3}	3.1522×10^{-2}	1.4085×10^{-2}	6.6671×10^{-3}

Example 4.6. The modified Kawahara equation [54]

$$u_t + au^2u_x + bu_{xxx} - ku_{xxxxx} = 0, \quad (75)$$

with the exact solution

$$u(x, t) = A \operatorname{sech}^2 [B(x - Ct)], \quad (76)$$

where a, b, k are constants, and $A = -\frac{3b}{\sqrt{10ak}}$, $B = \frac{1}{2}\sqrt{\frac{b}{5k}}$, $C = \frac{4b^2}{25k}$.

In simulations, we set $a = b = k = 1$. The simulation is conducted in $[-30, 30]$ with $\Delta x = 0.1$, $\Delta t = 0.01, 0.001$ and 0.0001 . Table VI. gives the errors of numerical solution for different times. From the table it is also found that there is little difference between accuracy of two schemes.

Example 4.7. The Korteweg-de Vries-Kawahara equation [44]

$$u_t + uu_x + u_x + u_{xxx} - u_{xxxxx} = 0, \quad (77)$$

with the exact solution

$$u(x, t) = \frac{105}{169} \operatorname{sech}^4 \left(\frac{1}{2\sqrt{13}}(x - \frac{205}{169}t - x_0) \right), \quad (78)$$

where x_0 is a parameter.

In simulations, we set $x_0 = 20$ as in Ref. [44]. The simulation is conducted in $[0, 200]$ with $\Delta x = 0.1$, $\Delta t = 0.01, 0.001$ and 0.0001 . Table VII. gives the errors of numerical solution for different times. It can be found that the numerical solutions obtained by LBGK model are in good agreement with the analytic ones. From the table it is still found that there is little difference between accuracy of two schemes.

The last two test problems are the third-order KdV-type equations. We use the D1Q5 LBGK model to simulate them. Similar to the above three test problems, we also compare the present *exact* model with C-E expansion to order $O(\epsilon^4)$ with one to order $O(\epsilon^3)$, and denote scheme 1 and scheme 2 for the model of order $O(\epsilon^4)$ and that of order $O(\epsilon^3)$, respectively. For simplification, we only take $\bar{\Pi}_4 = 0$ in Eq. (51) for scheme 2 in simulations.

Example 4.8. The KdV Burgers equation [20]

$$u_t + \alpha uu_x - \gamma u_{xx} + \delta u_{xxx} = 0, \quad (79)$$

with the exact solution

$$u(x, t) = 2\xi \left(1 - \frac{1}{[1 + e^{2\nu(x-\xi t)}]^2} \right), \quad (80)$$

where $\nu = -\frac{\gamma}{10\delta}$ and $\xi = \frac{6\gamma^2}{25\delta}$.

TABLE VIII: Comparison of global relative errors for $c = 1$ at different times [(1) Scheme 1; (2) Scheme 2; (3) Scheme in Ref. [49]].

τ_{opt}		$t = 10$	$t = 50$	$t = 150$	$t = 250$	$t = 300$
0.97	(1)	2.4300×10^{-6}	4.2738×10^{-6}	4.0518×10^{-6}	3.4676×10^{-6}	3.3242×10^{-6}
0.96	(2)	4.9172×10^{-6}	7.1775×10^{-6}	6.1615×10^{-6}	5.2459×10^{-6}	4.9383×10^{-6}
0.968	(3)	1.0416×10^{-5}	1.8801×10^{-5}	1.7409×10^{-5}	1.4877×10^{-5}	1.3901×10^{-5}

TABLE IX: Comparison of global relative errors for $c = 10$ at different times.

τ_{opt}		$t = 1$	$t = 2$	$t = 3$	$t = 4$
37.77	Scheme 1	1.8629×10^{-3}	9.1678×10^{-4}	9.2998×10^{-4}	7.1608×10^{-4}
31.52	Scheme 2	2.6472×10^{-2}	1.0947×10^{-2}	6.1720×10^{-3}	3.3151×10^{-3}

In simulations, we set $\alpha = 1, \gamma = 9 \times 10^{-4}, \delta = 2 \times 10^{-5}$, and the simulation is conducted in $[-4, 4]$ with $\Delta x = \Delta t = 0.01$ as in Refs. [20] and [49]. Table VIII. gives the errors of numerical solution for different times. From the table it is found that the errors of schemes 1 and 2 are much smaller than those of the model in Ref. [49], and scheme 1 is better than scheme 2, but there is little difference between our schemes. The numerical results show that the model in Ref. [49] is not exact, even for the constraints on lower-order moments.

Example 4.9. The $K(n, n)$ -Burgers equation [55]

$$u_t + a(u^n)_x + b(u^n)_{xxx} + ku_{xx} = 0, \quad (81)$$

with the exact solution

$$u(x, t) = [A(1 + \tanh(Bx + Ct))]^{-\frac{1}{n-1}}, b > 0, n > 1, a < 0 \quad (82)$$

where a, b, k, n are constants, and $A = \frac{1}{2k} \sqrt{-ab}, B = -\frac{n-1}{2n} \sqrt{-\frac{a}{b}}, C = \frac{ak(n-1)}{2bn}$.

In simulations, we set $a = -1, b = 1, k = -1, n = 2$. The simulation is conducted in $[-1, 1]$ with $\Delta x = 0.01, \Delta t = 0.001$. Table IX. gives the errors of numerical solution for different times. From the table it is found that the errors of schemes 1 are much smaller than those of scheme 2, which implies that for this problem the accuracy of higher-order model is much better than that of lower-order one.

V. CONCLUSION

In the present work, we have developed a unified LBGK model for 1D higher-order NPDEs. Through C-E expansion a given NPDE can be exactly recovered to required order of small parameter ϵ by choosing correct auxiliary moments. Unlike traditional numerical methods which solve for macroscopic variables, the model has the advantages of standard LBGK model, which are borrowed from kinetic theory, such as linearity of the convection operator in velocity space, simplicity and symmetry of scheme, ease in coding and intrinsical parallelism [3]. Detailed numerical tests of the proposed model are carried out for different types of NPDEs, including the Kuramoto-Sivashinsky type equations, Kawahara type equations, and KdV type equations. It is found that the simulation results agree well with the analytical and numerical solutions reported in previous studies, which shows that the LBM has potentials in simulating higher-order NPDEs. However, perhaps due to the effects of nonlinearity and higher order differentials, the LBGK model for solving higher order NPDEs is sensitive to the key parameters, such as $\Delta x, \Delta t$ and τ , and it does not seem so efficient as that for solving lower order ones, such as that for NCDEs [39].

Note that the proposed model can be directly applied to derive the LBGK model for high-order NPDEs in higher dimensional space by treating moments as tensors, and the LBGK model for NPDEs with order larger than six can be easily derived by using the idea in this paper. Nevertheless, some important issues, such as how to improve the accuracy and stability of the LB models need further studies.

Acknowledgments

This work is supported by the National Science Foundation of China (Grants No. 60773195 and No. 50606012).

-
- [1] R. Benzi, S. Succi, and M. Vergassola, The lattice Boltzmann equation: theory and applications, *Phys. Rep.* **222**, 145-197 (1992).
 - [2] Y. H. Qian, S. Succi, and S. A. Orszag, Recent advances in lattice Boltzmann computing, *Annu. Rev. Comput. Phys.* **3**, 195-242 (1995).
 - [3] S. Chen and G. D. Doolen, Lattice Boltzmann method for fluid flows, *Annu. Rev. Fluid Mech.* **30**, 329-364 (1998).
 - [4] F. J. Higuera, S. Succi, and R. Benzi, Lattice gas dynamics with enhanced collisions, *Europhys. Lett.* **9**, 345-349 (1989)
 - [5] D. d'Humières, Generalized lattice Boltzmann equations, in *Rarefied Gas Dynamics: Theory and Simulations*, edited by B. D. Shizgal and D. P. Weaver, *Progress in Astronautics and Aeronautics Vol. 159* (AIAA, Washington, DC, 1992), pp. 450-458.
 - [6] P. Lallemand and L.-S. Luo, Theory of the lattice Boltzmann method: Dispersion, dissipation, isotropy, Galilean invariance, and stability, *Phys. Rev. E* **61**, 6546-6562 (2000).
 - [7] I. V. Karlin, A. Ferrante, and H. C. Ottinger, Perfect entropy functions of the Lattice Boltzmann method, *Europhys. Lett.* **47**, 182-188 (1999).
 - [8] S. Ansumali, I. V. Karlin, and H. C. Ottinger, Minimal entropic kinetic models for hydrodynamics, *Europhys. Lett.* **63**, 798-804 (2003)
 - [9] S. S. Chikatamarla, S. Ansumali, and I. V. Karlin, Entropic lattice Boltzmann models for hydrodynamics in three dimensions, *Phys. Rev. Lett.* **97**, 010201 (2006).
 - [10] B. M. Boghosian, J. Yepez, P. V. Coveney, and A. Wagner, Entropic lattice Boltzmann methods, *Proc. R. Soc. London, Ser. A* **457**, 717-766 (2001).
 - [11] B. Keating, G. Vahala, J. Yepez, et al., Entropic lattice Boltzmann representations required to recover Navier-Stokes flows, *Phys. Rev. E* **75**, 036712 (2007)
 - [12] S. P. Dawson, S. Y. Chen, and G. D. Doolen, Lattice Boltzmann computations for reaction-diffusion equations, *J. Chem. Phys.* **98**, 1514-1523 (1993).
 - [13] R. Blaak and P. M. Sloot, Lattice dependence of reaction-diffusion in lattice Boltzmann modeling, *Comput. Phys. Comm.* **129**, 256-266 (2000).
 - [14] X. M. Yu and B. C. Shi, A lattice Boltzmann model for reaction dynamical systems with time delay, *Appl. Math. Comput.* **181**, 958-965 (2006).
 - [15] M. R. Swift, E. Orlandini, W. R. Osborn, and J. M. Yeomans, Lattice Boltzmann simulations of liquid-gas and binary fluid systems, *Phys. Rev. E* **54**, 5041-5052 (1996).
 - [16] Z. L. Guo, B. C. Shi, and N. C. Wang, Fully Lagrangian and lattice Boltzmann methods for the advection-diffusion equation, *J. Sci. Comput.* **14**(3), 291-300 (1999).
 - [17] X. Y. He, N. Li, and B. Goldstein, Lattice Boltzmann simulation of diffusion-convection systems with surface chemical reaction, *Mol. Simulat.* **25**, 145-156 (2000).
 - [18] B. C. Shi, B. Deng, R. Du, and X. W. Chen, A new scheme for source term in LBGK model for convection-diffusion equation, *Comput. Math. Appl.* **55**, 1568-1575 (2008).
 - [19] X. M. Yu and B. C. Shi, A lattice Bhatnagar-Gross-Krook model for a class of the generalized Burgers equations, *Chin. Phys.* **15**, 1441-1449 (2006).
 - [20] Z. H. Chai, B. C. Shi and L. Zheng, A unified lattice Boltzmann model for some nonlinear partial differential equations, *Chaos, Solitons and Fractals* **36**, 874-882 (2008).
 - [21] Z. H. Chai and B. C. Shi, A novel lattice Boltzmann model for the Poisson equation, *Appl. Math. Model.* **32**, 2050-2058 (2008).
 - [22] R. G. M. van der Sman and M. H. Ernst, Convection-diffusion lattice Boltzmann scheme for irregular lattices, *J. Comput. Phys.* **160**, 766-782 (2000).
 - [23] R. G. M. van der Sman, Galilean invariant lattice Boltzmann scheme for natural convection on square and rectangular lattices, *Phys. Rev. E* **74**, 026705 (2006).
 - [24] X. X. Zhang, A. G. Bengough, J. W. Crawford, and I. M. Young, A lattice BGK model for advection and anisotropic dispersion equation, *Adv. Water Resour.* **25**, 1-8 (2002).
 - [25] I. Rasin, S. Succi, and W. Miller, A multi-relaxation lattice kinetic method for passive scalar diffusion, *J. Comput. Phys.* **206**, 453-462 (2005).
 - [26] I. Ginzburg, Equilibrium-type and link-type lattice Boltzmann models for generic advection and anisotropic-dispersion equation, *Adv. Water Resour.* **28**, 1171-1195 (2005).
 - [27] D. A. Meyer, From quantum cellular automata to quantum lattice gases, *J. Stat. Phys.* **85**, 551-574 (1996).
 - [28] S. Succi and R. Benzi, Lattice Boltzmann equation for quantum mechanics, *Physica D* **69**, 327-332 (1993).
 - [29] S. Succi, Numerical solution of the Schrödinger equation using discrete kinetic theory, *Phys. Rev. E* **53**, 1969-1975 (1996).
 - [30] B. Boghosian and W. Taylor IV, Quantum lattice-gas models for the many-body Schrödinger equation, *Int. J. Mod. Phys. C* **8**, 705-716 (1997).

- [31] J. Yepez and B. Boghosian, An efficient and accurate quantum lattice-gas model for the many-body Schrodinger wave equation, *Comput. Phys. Commun.* **146**, 280-294 (2002).
- [32] J. Yepez, Quantum lattice-gas model for the Burgers equation, *J. Stat. Phys.* **107**, 203-224 (2002).
- [33] G. Vahala, J. Yepez, and L. Vahala, Quantum lattice gas representation of some classical solitons, *Phys. Lett. A* **310**, 187-196 (2003).
- [34] G. Vahala, L. Vahala, and J. Yepez, Quantum lattice representations for vector solitons in external potentials, *Physica A* **362**, 215-221 (2006).
- [35] S. Palpacelli and S. Succi, Numerical validation of the quantum lattice Boltzmann scheme in two and three dimensions, *Phys. Rev. E* **75**, 066704 (2007); Quantum lattice Boltzmann simulation of expanding Bose-Einstein condensates in random potentials, *Phys. Rev. E* **77**, 066708 (2008).
- [36] S. Palpacelli and S. Succi, The quantum lattice Boltzmann equation: Recent developments, *Commun. Comput. Phys.* **4**, 980-1007 (2008).
- [37] L. H. Zhong, S. D. Feng, P. Dong, and S. T. Gao, Lattice Boltzmann schemes for the nonlinear Schrödinger equation, *Phys. Rev. E* **74**, 036704 (2006).
- [38] B. C. Shi, Lattice Boltzmann simulation of some nonlinear complex equations, *Lect. Notes Comput. Sci.* **4487**, 818-825 (2007).
- [39] B. C. Shi and Z. L. Guo, Lattice Boltzmann model for nonlinear convection-diffusion equations, *Phys. Rev. E* **79**, 016701 (2009).
- [40] B. C. Shi and Z. L. Guo, Lattice Boltzmann model for the one-dimensional nonlinear Dirac equation, *Phys. Rev. E* **79**, 066704 (2009).
- [41] M.A. Lopez-Marcos, Numerical analysis of pseudospectral method for the Kuramoto-Sivashinsky equation, *IMA J. Numer. Anal.* **14**, 223-242 (1994).
- [42] Y. Xu and C.-W. Shu, Local discontinuous Galerkin methods for the Kuramoto-Sivashinsky equations and the Ito-type coupled KdV equations, *Comput. Methods Appl. Mech. Engrg.* **195**, 3430 (2006).
- [43] Y. Xu and C.-W. Shu, Local discontinuous Galerkin methods for high-order time-dependent partial differential equations, *Commun. Comput. Phys.* **7**, 1-46 (2010).
- [44] J. C. Ceballos, M. Sepúlveda, and O. P. V. Villagrán, The Korteweg-de Vries-Kawahara equation in a bounded domain and some numerical results, *Appl. Math. Comput.* **190**, 912-936 (2007).
- [45] L. Cueto-Felgueroso and J. Peraire, A time-adaptive finite volume method for the Cahn-Hilliard and Kuramoto-Sivashinsky equations, *J. Comput. Phys.* **227**, 9985-10017 (2008).
- [46] Marjan Uddin, S. Haq and Siraj-ul-Islam, A mesh-free numerical method for solution of the family of Kuramoto-Sivashinsky equations, *Appl. Math. Comput.* **212**, 458-469 (2009).
- [47] J. Y. Zhang and G. W. Yan, Lattice Boltzmann method for one and two-dimensional Burgers equation, *Physica A* **387**, 4771-4786 (2008).
- [48] B. Servan-Camas and F. T.-C. Tsai, Lattice Boltzmann method with two relaxation times for advection-diffusion equation: Third order analysis and stability analysis, *Adv. Water Resour.* **31**, 1113-1126 (2008).
- [49] H. L. Lai and C. F. Ma, A higher order lattice BGK model for simulating some nonlinear partial differential equations, *Sci. China Ser. G* **52**, 1053-1061 (2009).
- [50] H. L. Lai and C. F. Ma, Lattice Boltzmann method for the generalized Kuramoto-Sivashinsky equation, *Physica A* **388**, 1405-1412 (2009).
- [51] Z. L. Guo, C. G. Zheng, and B. C. Shi, Non-equilibrium extrapolation method for velocity and pressure boundary conditions in the lattice Boltzmann method, *Chin. Phys.* **11**, 366-374 (2002).
- [52] J. W. Zhang and J. G. Zhang, Exact solutions of the generalized Kuramoto-Sivashinsky type equations with the dispersive effects (in Chinese), *Math. Pract. Theor.*, **31**, 427-429 (2001).
- [53] A.-M. Wazwaz, New solitary wave solutions to the Kuramoto-Sivashinsky and the Kawahara equations, *Appl. Math. Comput.* **182**, 1642-1650 (2006).
- [54] A.-M. Wazwaz, New solitary wave solutions to the modified Kawahara equation, *Phys. Lett. A* **360**, 588-592 (2007).
- [55] A.-M. Wazwaz, The tanh method for compact and noncompact solutions for variants of the KdV-Burger and the $K(n,n)$ -Burger equations, *Physica D*, **213**, 147-151 (2006).